Paper presented at the 6th International School on Physics of Exotic Atoms, Erice, Mar 21 - 30

TRI-PP-94-73
Aug 1994

MEASUREMENT OF THE INDUCED PSEUDOSCALAR COUPLING VIA RADIATIVE MUON CAPTURE ON HYDROGEN

RMC Collaboration:

M.D. Hasinoff, C.Q. Chen, P. Gumplinger, A.J. Larabee*, E. Saettler, D.G. Sample, S. Veillette
University of British Columbia, Vancouver, British Columbia, V6T 1Z1 Canada

G. Azuelos, J.A. Macdonald, J.-M. Poutissou, R. Poutissou, D.H. Wright
TRIUMF, Vancouver, British Columbia, V6T 2A3 Canada

G. Azuelos, P . Depommier, B. Doyle, G. Jonkmans
Université de Montréal, Montréal, Québec H3C 3J7 Canada

D.S. Armstrong†, M. Blecher, C.M. Sigler,
Virginia Polytechnic Institute & State University, Blacksburg, VA 24061 USA

S.C. McDonald, M. Munro, G.N. Taylor
University of Melbourne, Parkville, Victoria 3001 Australia

W. Bertl
Paul Scherrer Institute, CH-5232 Villigen, Switzerland

T.P. Gorringe
University of Kentucky, Lexington, Kentucky, 40506 USA

B.C. Robertson
Queen's University, Kingston, Ontario, K7L 3N6 Canada

ABSTRACT

The hydrogen atom is the most fundamental lepton-hadron system and it has been used very extensively to test our theories of the electroweak interaction. Muonic hydrogen, $\mu^- p$, is the next most fundamental atom and therefore it can also be used to test and extend our basic knowledge of the electroweak interaction between leptons and quarks. Both the ordinary muon capture (OMC) reaction, $\mu^- p \rightarrow \nu_\mu n$, and the radiative muon capture (RMC) reaction, $\mu^- p \rightarrow \nu_\mu n \gamma$, are sensitive to g_P, the induced pseudoscalar coupling constant of the semi-leptonic interaction. However, RMC is considerably more sensitive to g_P because of the much larger range of momentum transfers which can occur in the RMC reaction. For the highest photon energies the RMC pseudoscalar amplitude is enhanced by more than a factor of three. A status report and preliminary results from TRIUMF Experiment 452, radiative muon capture on hydrogen, are presented in this paper.

*Present address, Buena Vista College, Storm Lake, Iowa 50588 USA
†Present address, College of William & Mary, Williamsburg, VA 23185 USA

1. INTRODUCTION

Muon decay and muon capture involve significantly larger momentum transfers than nuclear beta decay or electron capture. Consequently, these low energy muon reactions provide us with new information about the weak interaction. The μ capture reaction involves one hadron and one lepton. Therefore, it includes contributions from both the lepton and the quark currents and so its study is even richer than that of μ decay. However, the capture rate is considerably smaller ($\Lambda_{\rm OMC}/\Lambda_{\rm decay} \sim 10^{-3}$) and so the μ capture experiments are correspondingly more difficult. In my lectures here at Erice I will discuss the RMC experiment currently underway at TRIUMF. The radiative muon capture rate is extremely small ($\Lambda_{\rm RMC}/\Lambda_{\rm decay} \sim 10^{-8}$) so that an elaborate detector and background suppression system is necessary for its observation. We actually began our TRIUMF RMC experiments in 1985 using nuclear targets, where the branching ratios ($\Lambda_{\rm RMC}/\Lambda_{\rm decay} \sim 2\times10^{-5}$) are considerably larger. For a detector which was insensitive to neutrons we used the TRIUMF TPC, suitably modified into a cylindrical pair spectrometer by the addition of a lead converter. By 1987 we realized that we could not measure RMC(H) in this multiplexed detector and so we began building a new fully de-multiplexed drift chamber tracking detector. We started data collection on hydrogen in Aug. '90 and have now accumulated nearly 90 days of beam time at the rate of ~30 days/year. With a μ^- stopping rate of ~ 700 K/s we observe only ~4 good RMC events/day. During this talk I will explain the various experimental difficulties we have had to overcome and present our preliminary results for g_P.

2. PHYSICS BACKGROUND

The standard model of electroweak interactions describes muon capture at the lepton-quark level. At low energies, this Hamiltonian can be reduced to a four-fermion contact interaction with the $V-A$ form:

$$H = \frac{G_F}{\sqrt{2}} \; \bar{d}\gamma^\mu(1-\gamma^5)u \quad \bar{\nu}_\mu\gamma_\mu(1-\gamma^5)\mu \qquad (1)$$

However, quarks do not exist in the free state, and therefore we can only observe muon capture at the lepton-hadron level. Here, the situation is considerably more complicated, due to the presence of the strong interaction. The latter is believed to be described by quantum chromodynamics, but this theory is not very predictive in the non-perturbative regime at low energy. Traditionally, one parametrizes the hadronic matrix elements in terms of form factors, which are functions of the momentum transfer squared. Using standard notations,[1] we have, for the hadronic

matrix elements of the vector and axial-vector matrix elements:

$$< n|V_\mu|p > = \bar{u}_n\Big[F_V(q^2)\gamma_\mu + F_M(q^2)\frac{1}{2M}\sigma_{\mu\nu}q^\nu + \frac{1}{m_l}F_S(q^2)q_\mu\Big]u_p \quad (2)$$

$$< n|A_\mu|p > = \bar{u}_n\Big[F_A(q^2)\gamma_\mu\gamma^5 + F_T(q^2)\frac{1}{2M}\sigma_{\mu\nu}\gamma^5 q^\nu + \frac{1}{m_l}F_P(q^2)\gamma^5 q_\mu\Big]u_p \quad (3)$$

where M is the nucleon mass, m_l is the lepton mass and u_p and $\bar{u}_n$ are Dirac spinors.

The standard model, along with symmetry arguments and the available experimental results allow us to reduce the number of unknown form factors as follows:

- The standard model does not predict the existence of second-class currents; therefore we take $F_S(q^2) \equiv 0$ and $F_T(q^2) \equiv 0$.
- Assuming time-reversal invariance in the first generation of quarks and leptons, all form factors can be chosen as real functions.
- Using the conservation of the vector current (CVC), which is an ingredient of the standard model, one relates the form factors $F_V(q^2)$ and $F_M(q^2)$ to the electromagnetic form factors, which are well measured by electron scattering.
- The β decay of the neutron provides us with a value of $F_A(q^2 = 0)$. The q^2 dependence of $F_A(q^2)$ is known from experiment.[2-5] For our purpose this is a small effect.

Therefore we are left with the pseudoscalar form factor, $F_P(q^2)$, which is the subject of our experimental study. This form factor has been studied theoretically in the context of the partial conservation of axial current (PCAC hypothesis) where the pion plays a very special role. Using additional assumptions on the q^2 dependence of the form factors, one gets the Goldberger-Treiman relation for g_P*:

$$g_P(q^2) = \frac{2m_\mu g_{\pi NN} F_\pi}{m_\pi^2 + q^2} = \ldots g_A(q^2) \quad (4)$$

where $g_{\pi NN}$ is the pion-nucleon coupling constant and F_π is the pion decay constant. According to a recent experimental result[5] this momentum-transfer dependence of g_P is well described by the pion-pole dominance.

Using as input values the well-known masses m_π, m_μ and M, and:

$$\begin{aligned} F_\pi &= (92.5 \pm 0.2)\,\text{MeV} \\ g_A &= 1.2573 \pm 0.0028 \\ g_{\pi NN} &= 13.31 \pm 0.34 \end{aligned} \quad (5a)$$

*The use of coupling constants, g_i, rather than form factors, F_i, is preferred in this case, since the momentum dependence is small, except for g_P . The form factors are related to the coupling constants as follows: $g_{V,A} = F_{V,A}$, $g_{M,T} = 2\cdot M\cdot F_{M,T}$, $g_{P,S} = m_\mu \cdot F_{P,S}$ where M and m_μ are the nucleon and muon masses, respectively.

we obtain

$$g_P(0.88m_\mu^2) = 7.1 g_A(0) \quad (5b)$$

The choice of $q^2 = 0.88m_\mu^2$ corresponds to the fact that the momentum transfer in OMC has this particular value.

A new calculation[6] of g_P has appeared recently. It is based on the chiral Ward identities of QCD and heavy-baryon chiral perturbation theory:

$$g_P = \frac{2m_\mu g_{\pi NN} F_\pi}{m_\pi^2 + 0.88m_\mu^2} - \frac{1}{3}g_A m_\mu M r_A^2 \quad (6)$$

where r_A^2 is the mean square axial radius of the nucleon. This result was first presented by Wolfenstein,[7,8] using a once-subtracted dispersion relation. However, this QCD derivation now places it on much firmer theoretical ground.

With

$$r_A = (0.65 \pm 0.03)\,\text{fm} = (3.30 \pm 0.15)\,\text{GeV}^{-1} \quad (7a)$$

one obtains[6]:

$$g_P = (8.89 \pm 0.23) - (0.45 \pm 0.04) = 8.44 \pm 0.23 \quad (7b)$$

Considering the accuracy of this theoretical prediction, it is urgent to measure g_P to an accuracy of 2%. However, as I mentioned earlier in the introduction, the branching ratio for RMC(H) is extremely small ($\sim 10^{-8}$), consequently it has never been observed before. The current TRIUMF experiment seeks to observe the RMC(H) process for the first time and hopes to reduce the error on g_P from the 42% obtained in the best OMC experiment[9] down to ~10%.

The RMC rate is considerably more sensitive to g_P than the OMC rate. This increased sensitivity arises because of the variable momentum transfer, which can even become *time-like* for the highest photon energies. However, the extremely low RMC(H) branching ratio has thus far limited studies to nuclear targets where additional complications due to nuclear structure also arise. There is also the possibility, very interesting in its own right, that g_P is modified inside the nucleus due to a renormalization of the nucleon's pion cloud within the nuclear medium.[10,11] The most recent nuclear RMC measurements[12,13] seem to show a decrease of g_P with increasing Z but the data[14,15] for ^{16}O can be well described by the PCAC value for g_P if one uses a phenomenological nuclear model[16] or by an enhanced g_P value nearly twice as large as the PCAC prediction when using a microscopic nuclear shell model.[17] The larger g_P value is in good agreement with the value obtained from a comparison[18] of OMC on ^{16}O to the $0^- \rightarrow 0^+$ β-decay of ^{16}N

which gives $g_P/g_A \simeq 12.5$. Thus, in addition to providing a test of PCAC and the dominance of the pion pole, the elementary hydrogen measurement to be discussed below can also serve as a benchmark for testing such basic ideas as renormalization of the nucleon size and coupling strength inside nuclei.

The theory of RMC has been developed by several[19–22] authors. RMC on hydrogen was first calculated by Huang, *et al.*,[19] although it was the work of Opat[20] which first included the hyperfine effects in the singlet or triplet μp atomic states, as well as in the spin-doublet ortho $[p\mu p]$ molecular state. The expected RMC sensitivity to g_P was predicted to be nearly equal to the accuracy in the rate determination; unlike the case for OMC where a 4% rate measurement leads to a 42% error in g_P. The most recent calculation of Beder and Fearing[23] included the contribution of Δ excitation and concluded that the effect is at most 8% at the highest photon energies. Since we are forced to use a liquid H_2 target in order to stop enough μ's the muonic chemistry is complicated. The ortho-molecular state can decay ($\lambda_{op} = 4.1 \pm 1.4 \times 10^4$ s^{-1}) into the para-molecular state, which has a somewhat larger RMC rate. Figure 1 shows the relative contributions, $G_i(t)$, to the total RMC rate in liquid H_2 from the singlet μp atom and the two $p\mu p$ molecular states. The RMC rate is dominated by the ortho-molecular state only for the first few μ^- lifetimes so that the para-molecular contribution (about 20% of the total RMC rate) cannot be ignored. In the OMC case[9] the non-zero ortho-para conversion rate produces a change in the g_P/g_A value from 13.8 ± 2.0 for the case λ_{op}=0 down to 7.1 ± 3.0 when $\lambda_{op} = 4.1 \pm 1.4 \times 10^4$ s^{-1}. The RMC(H) rate, on the other hand, is relatively insensitive to the exact value of λ_{op} as shown in Fig. 2.

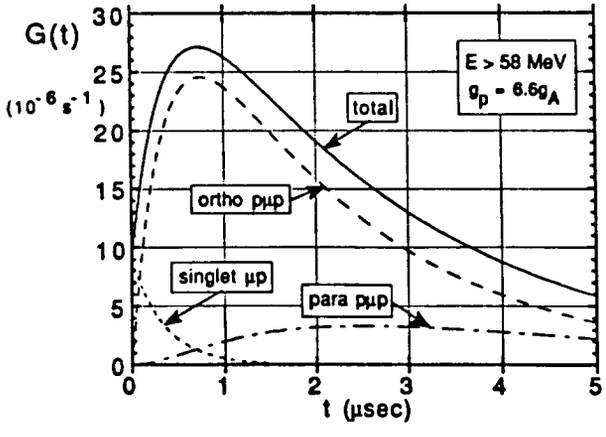

Fig. 1. RMC time distributions in liquid H_2. $G_i(t)$ is the product of the relative populations, $P_i(t)$, and the RMC rates, Γ_i, for each state.[23]

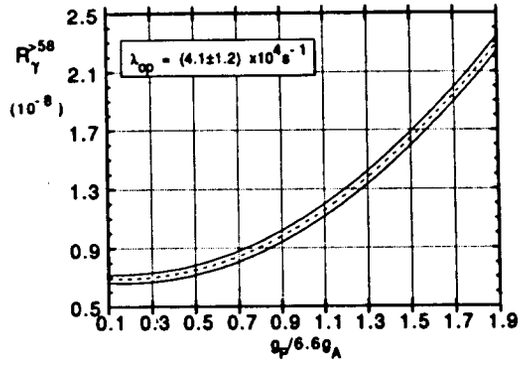

Fig. 2. The branching ratio (E_γ > 58 MeV) for RMC as a function of g_P/g_A for the measured value of the ortho-para conversion rate.[23]

3. EXPERIMENTAL DIFFICULTIES

- **Hydrogen Purity**— An extremely high purity of the hydrogen in the liquid is critical, otherwise the μ^- will be stolen from the proton before capture can take place. Impurity levels of $< 10^{-9}$ for all elements other than hydrogen are necessary since the capture probability increases as Z^4_{eff} while the branching ratio for RMC/OMC (E_γ > 58 MeV) decreases only very slowly with increasing Z. Such purity is achieved by passing the hydrogen gas through a palladium filter each time it is transferred into the target vessel which itself is carefully outgassed for a period of at least 14 days prior to each run. An outgassing rate of $\approx 5 \times 10^{-11}$ l/min for the gold-walled cell has been achieved; this accumulates to $\approx 2 \times 10^{-6}$ liters in 30 days.† To reduce the formation of $p\mu d^+$ molecules and then ^{3}He by μ-induced fusion, the natural concentration (100–150 ppm) of deuterium in hydrogen was reduced to <2.0 ppm by electrolyzing hydrogen from deuterium-depleted water‡. At this level the probability of RMC on ^{3}He is reduced to $\approx$ 2% of the hydrogen RMC signal level.

- **Hydrogen Target**— Even though the RMC probability increases rapidly with Z, we chose Au for the target wall material. This decision was based on extensive Monte Carlo simulations and detailed measurements of the stopping distribution of the muon beam. The dimensions of the cylindrical Au

†The outgassing rate at LH_2 temperatures is several orders of magnitude lower than that at room temperature so this estimate is a conservative upper limit for the heavy impurities.

‡Manufactured by AECL-Canada, Chalk River, Ontario K0J 1J0 Canada

flask were 16 cm ϕ × 15 cm length × 250 μ thickness. The heat shields, made of 30 μ Ag were designed to insure that any muons scattered at large angles from the beam counters would not be stopped in the region of the Au target walls. The RMC events from Au or Ag can be nearly eliminated by exploiting the short capture time (73 ns, 89 ns) in Au and Ag, respectively by imposing a blanking time of cut $5\tau_{\mu}^{Au}$= 365 ns following each μ-stop as well as by tracking cuts to select events originating in the hydrogen fiducial volume. Diffusion of $p\mu p$ atoms to the walls has been estimated but this is not expected to be a problem in such a large volume LH_2 target.

- **Bremsstrahlung**— The unavoidable backgrounds of both internal and external bremsstrahlung from ordinary muon decay electrons can only occur below E_γ= 53 MeV. Because of the finite energy resolution of the spectrometer we are forced to place our low energy cutoff at 58 MeV. A check of the high energy response function of the spectrometer can be obtained from a comparison of the μ^+ and μ^- radiative muon decay (RMD) processes after a subtraction of the substantial contribution from the annihilation of the decay e^+ in the μ^+ RMD case. The magnitude of this annihilation component is compared with the bremsstrahlung and radiative decay terms in Fig. 3.

- **Prompt Photons**— Gammas from the decays of π^0's produced by charge exchange (B.R. $\simeq$ 0.6) from the few pions ($< 10^{-3}$) remaining in the muon beam after the rf separator occur exactly in the energy region of the RMC signal. The beam counters range out nearly 90% of the surviving pions but those remaining can produce prompt γ's. However, these can be easily eliminated (well below the 10^{-10} level) by rejecting any events which are in prompt time coincidence with a beam particle or where the pulse-height in any of the four beam counters is non-zero.

- **Spurious Photons**— Falsely reconstructed photons from the pile-up of a decay e^- with an e^+ from a very asymmetric photon conversion in the Pb converter during the drift time of the tracks in the drift chamber must also be accurately identified and rejected. Since we have the multi-hit timing information available from the trigger scintillators this is easily done off-line in software.

- **Cosmic Ray and Cyclotron Background**— Even cosmic-ray induced photons constitute a potentially troublesome background. The entire detector is therefore covered on the top and sides with both scintillators and drift chambers to reject such events. In addition, the use of a tracking detector with multi-hit capabilities allows rejection of any γ event in which there is any additional track indicating the presence of an initiating cosmic ray shower.

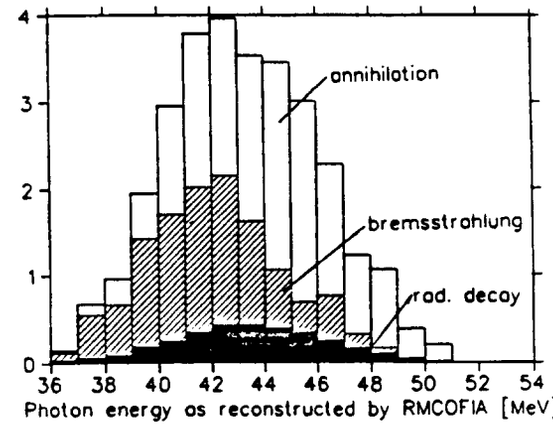

Fig. 3. Individual contributions to the low energy gamma spectrum for μ^+ decay indicating the very substantial contribution of the e^+ annihilation. All spectra have been folded with the RMC spectrometer acceptance and response functions to compare directly with the experimental data.

We have accumulated substantial beam-off data in order to characterize and measure this true cr background. We have also collected considerable beam-on background data when the cyclotron is operating but beam is not being delivered to our channel and are able to identify a machine related gamma background in the region between 50-200 MeV.

4. TRIUMF RMC SPECTROMETER

Since the RMC process on hydrogen is so extremely rare (branching ratio for E_γ >58 MeV $\simeq 1.6 \times 10^{-8}$), it must be separated from the extremely large number of low energy γ's from RMD as mentioned above. A detector with a large solid angle, good detection efficiency and at least moderately good energy resolution is essential. The choice of a cylindrical ($\Omega \approx 3\pi$) pair spectrometer for a tracking detector provides a unique photon signature and thus completely eliminates the neutron problem which plagued the earlier nuclear RMC measurements with NaI detectors. A schematic view of the TRIUMF RMC facility is given in Fig. 4. The LH_2 target is surrounded by 5 polygonal assemblies of concentric segmented scintillators (A,A',B,C,D) which are used to form the fast first-level trigger and also to reject the single charged tracks from ordinary muon decay. A thin (1.08 mm) Pb converter is placed between the 12-fold segmented B/C scintillators. A proportional wire chamber (IWC) is inserted just inside the inner wall of the main drift chamber which has 4 superlayers (3 axial

and 1 stereo). The stereo layer provides one z point per track,while the second z point is provided by the IWC which has 2 layers of spiral cathodes. Each of the 6 sense wires in each of the 272 drift cells is connected to a multi-hit LeCroy 1879 FastbusTDC to measure the drift times in 2 ns buckets. A check on the trigger pattern from the C and D scintillators is made for the proper curvature of both $e^{\pm}$ tracks and then a minimum number of active drift cells in each of the super layers of the drift chamber is required in the second-level trigger within 1 μs. This second-level hardware trigger reduces the trigger rate from 1500 Hz to about 300 Hz. A third-trigger decision using software cuts in the Fastbus(SSP) microprocessor reduces the taping rate to less than 100 Hz with a typical event size of 2 Kbytes.

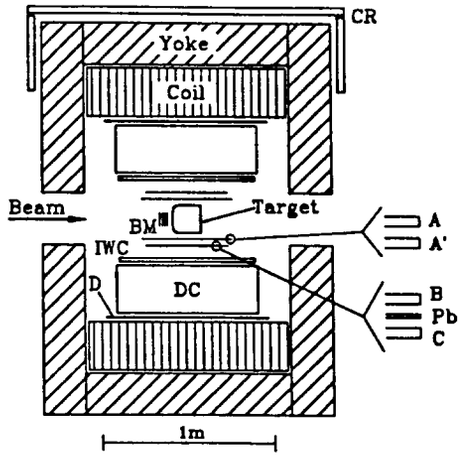

Fig. 4. Side view of the TRIUMF RMC spectrometer facility (see text for details).

5. PRELIMINARY RESULTS

Both the acceptance and the line shape of the spectrometer can be determined using the well known pion-induced reactions:

$$\pi^- p \rightarrow \gamma n \qquad 38.6\% \qquad\qquad \pi^- p \rightarrow \pi^0 n \rightarrow \gamma\gamma n \qquad 60.7\%$$

The first reaction gives a mono-energetic photon of 129 MeV while the second produces a flat spectrum for gamma energies between 55 and 83 MeV. A typical event where both of the π^0 gamma's have converted in the thin Pb sheet (10% conversion probability) is shown in Fig. 5. The overall spatial resolution for the $e^{\pm}$ tracks in the dc is $\approx$ 140μ and the spectrometer energy resolution for a 0.24 T magnetic field is $\approx$ 10% (FWHM) between 50 and 130 MeV. The major contributor to the energy resolution is multiple scattering in the drift chamber gas (Argon:Ethane, 50:50) followed by the energy loss in the Pb converter. Figure 6 shows the measured photon energy spectrum and the simulated Monte Carlo distribution; the agreement gives us confidence that we are modeling the detector correctly. Such $\pi^- p$ runs are taken at regular intervals during the course of the $\mu^- p$ data collection to monitor the acceptance of the spectrometer. The pion data are analyzed with exactly the same tracking and geometrical cuts as the muon-induced events.

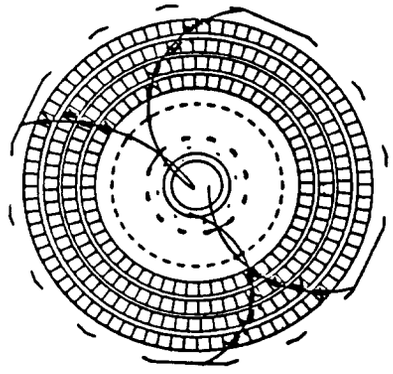

Fig. 5. End view of a 2γ conversion event from $\pi^0 \rightarrow \gamma\gamma$ decay. The hit scintillators are shown as solid lines.

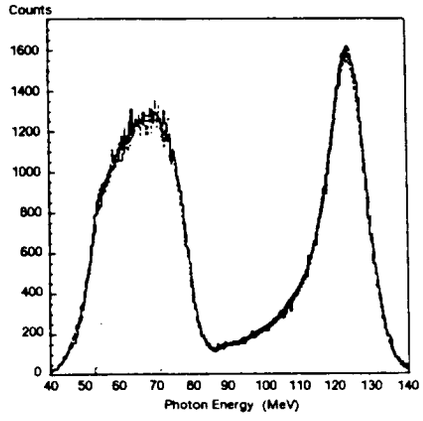

Fig. 6. Photon energy spectrum from the reactions $\pi^- p \rightarrow \gamma n$ and $\pi^- p \rightarrow \pi^0 n \rightarrow \gamma\gamma n$ compared with a Monte Carlo simulation (shaded area).

Knowing the number of pion stops (corrected for in-flight decays) it is relatively straightforward to evaluate the detection efficiency (acceptance) as a function of photon energy.

In order to obtain the final RMC(H) spectrum it is necessary to apply several software cuts (described in detail below) to the raw data.

Figure 7 shows the hydrogen RMC spectrum after application of the tracking and photon cuts which are used to select "possible" 2-track gamma events. Figure 8 shows the same spectrum after all the remaining software cuts have been applied.

- The **tracking** cut rejects tracks which are badly reconstructed— mainly due to multiple scattering in the drift chamber gas. It is quite effective in reducing the high-energy tail of the RMD and bremsstrahlung photon spectrum.
- The **photon** cut ensures that the e^+ and e^- track originate from the same point along the Pb converter. The energy spectrum is dominated by the RMD and bremsstrahlung events below 55 MeV and the prompt π^-p events above 55 MeV.
- The **prompt** cut rejects events in coincidence with a beam counter by testing both the TDC and ADC values; it totally removes the π^- induced gammas.
- Several **geometrical** cuts are used to insure that the γ event originates within the fiducial volume of the LH_2 target. In this way we reduce somewhat those γ's which originate in the Pb collimator and upstream Au target wall

or Ag heat shields. The cosmic-ray and machine-induced background is also reduced by these cuts.

- The **random** cut eliminates accidental coincidences of tracks which could fake good photons as discussed above.
- The **blanking time** cut is applied to reduce the rather large number of RMC photons produced in the materials surrounding the hydrogen (mainly Au and Ag) to a manageable number.

The few events observed in the spectrum above 100 MeV are roughly consistent with measurements of the background spectrum taken when the cyclotron is operating and delivering beam to the nearby channels. The true cosmic-ray photon background spectrum, measured when the cyclotron is off, accounts for about 65% of the measured rate between 100-200 MeV but only about 40% of the measured rate in the RMC signal region (58-100 MeV). We believe that this "machine related" gamma background is due to neutrons produced at the production target or beam dump which enter the spectrometer and produce γ's by (n,γ) or (n,π^0) reactions in the yoke or coil of the magnet. Further data are now being accumulated to reduce the error on this background subtraction.

The time distribution of gamma events passing all cuts except the blanking time cut is shown in Fig. 9. This spectrum indicates that most of the high energy photons ($E_\gamma > 58$ MeV) are actually produced from RMC on gold and silver rather than from hydrogen ($\Lambda_{capt} \approx Z^4_{eff}$) even though only a few % of the μ's actually

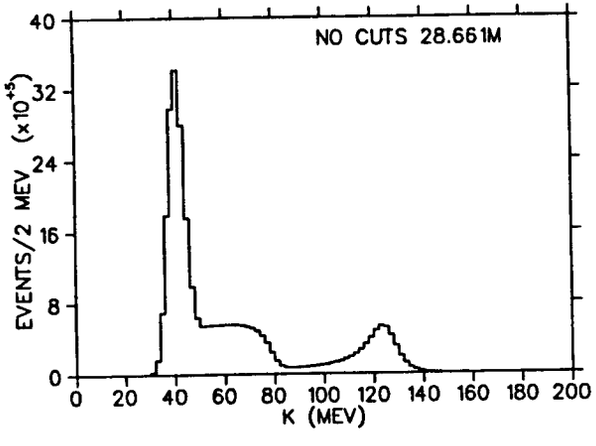

Fig. 7. Reconstructed RMC photon spectrum with no cuts applied except very general tracking and vertex requirements.

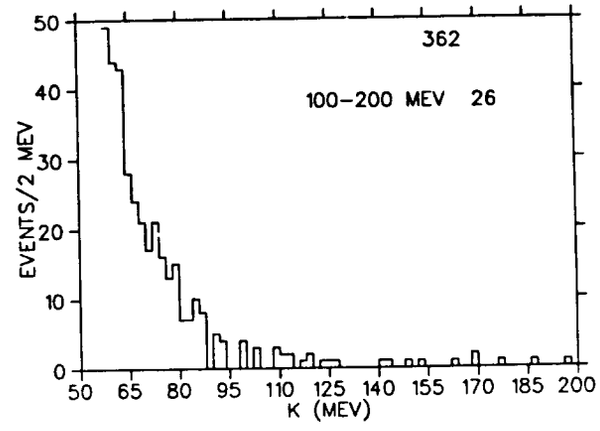

Fig. 8. Reconstructed RMC photon spectrum with all cuts applied (including the blanking time cut).

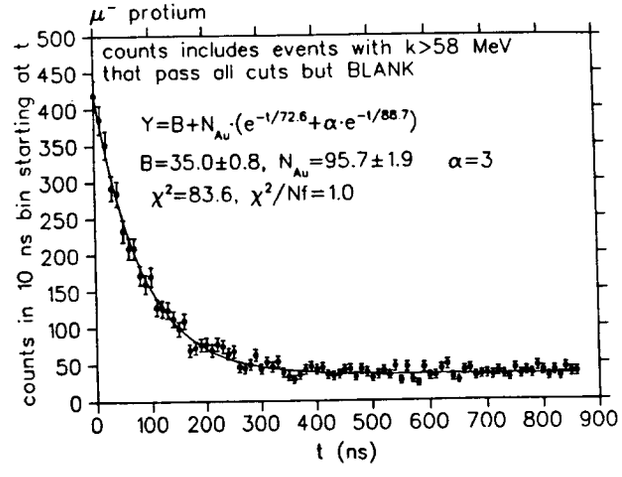

Fig. 9. Time distribution of all photon events with $E_\gamma > 58$ MeV which pass all cuts except the blanking time cut. The solid line is a fit to the data with 2 different lifetimes for Au and Ag plus a constant background to account for muon pileup.

stop in the gold target vessel or the silver heat shields. The solid curve is a fit with 2 exponentials ($\tau_\mu^{Au}, \tau_\mu^{Ag}$) plus a constant background to account for the pileup of 2 or more muons. The target background is not sensitive to the exact value chosen

for the constant, α. Hence it is set equal to the Monte Carlo prediction. From such a fit we can obtain the relative numbers of μ's stopping in LH_2 and Au and then extrapolate beyond $5\tau_{\mu}^{Au} = 365$ ns to obtain an estimate of the number of Au/Ag events in our final hydrogen RMC spectrum (71 events).

6. SUMMARY & OUTLOOK

The final hydrogen RMC spectrum contains 362 events with $E_\gamma > 58$ MeV. This represents all the data collected in 6 running periods between August '90 and July '92 ($\approx 3.1 \times 10^{12}$ μ^- stops). There are 336 events in the RMC region of the spectrum (58–100 MeV). After subtraction of the backgrounds from cosmic rays (15%), the Au/Ag wall stops (22%), the high energy tail of the bremsstrahlung γ's (5%), and $p\mu d$ fusion (1.0%), we obtain about 200 events with an overall statistical error of $\approx$ 12%. Runs with ordinary hydrogen gas with $\approx$ 100 ppm deuterium contamination have also been performed ($\approx 3.9 \times 10^{11}\mu$ stops) to check the calculated number of RMC photons expected from ^{3}He following $p\mu d$ fusion. The extraction of g_P/g_A from the measured RMC rate requires a careful determination of all of our systematic errors and verification of our Monte Carlo simulation (because of the finite energy resolution of the spectrometer). The preliminary[24] indications are a value for $g_P/g_A \sim 1.3$ times the PCAC prediction when using the experimental value for λ_{op}. However, this value is based on our current estimates for the number of μ's and π's which actually stop in the liquid hydrogen target. Further experimental checks on the stopping distributions are in progress. We have also accumulated data with even cleaner hydrogen gas (< 0.5 ppm D_2) since Jan '92. These newer data give a somewhat lower branching ratio and consequently a value for g_P/g_A considerably closer to the PCAC prediction. If a reanalysis of our gas samples confirms the initial purity measurements then there might be reason to question some of the muon chemistry transfer parameters. We expect to complete the analysis of all our data (including the recent Jan '94 data) by the end of 1994. The combined systematic errors are expected to be $\approx$10% excluding the 4% contribution due to the uncertainty in λ_{op}. When all the errors, including the λ_{op} uncertainty are combined with the final statistical error, we expect a 12% determination of the capture rate leading to a 15% value for g_P .

7. ACKNOWLEDGEMENTS

This work is supported by the Natural Sciences and Engineering Research Council (NSERC) and the National Research Council (NRC) of Canada, the U.S. National Science Foundation (NSF), the Paul Scherrer Institute (Switzerland) and the Australia Research Council.

8. REFERENCES

1. Mukhopadhyay, N.C., *Study of fundamental interactions with nuclear muon capture*, Proceedings of the International Conference on Weak and Electroweak Interactions in Nuclei (Montréal, May 1989) pg. 51, Ed. P. Depommier (Éditions Frontiéres, (1989)).
2. Delguerra, A., *et al.*, Nucl. Phys. **B107**, 65 (1976).
3. Esaulov, A.S., *et al.*, Nucl. Phys., **B136**, 511 (1978).
4. Ahrens, L.A., *et al.*, Phys. Lett., **B202**, 284 (1988).
5. Choi, S. *et al.*, Phys., Rev. Lett., **71**, 3927 (1993).
6. Bernard, V. *et al.*, "QCD accurately predicts the induced pseudoscalar coupling constant", Strasbourg Preprint CRN-94/13, (submitted for publication).
7. Wolfenstein, L., *High-Energy Physics and Nuclear Structure*, (Plenum, New York, (1970)), Pg. 661, ed. S. Devons.
8. Pagels, H. Phys. Rev. **179**, 1337 (1969).
9. Bardin, G. *et al.*, Phys. Lett, **104B**, 320 (1981).
10. Delorme, J. *et al.*, Ann. of Phys., **102**, 273 (1976).
11. Ericson, M., *Progress in Nuclear and Particle Physics*, (Pergamon, Oxford (1978)) pg. 67.
12. Dobeli, M. *et al.*, Phys. Rev. **C37**, 1633 (1988).
13. Armstrong, D.S. *et al.*, Phys. Rev., **C46**, 1094 (1992).
14. Armstrong, D.S. *et al.*, Phys. Rev., **C40**, R1100 (1989).
15. Armstrong, D.S. *et al.*, Phys. Rev., **C43** 1425 (1991).
16. Christillin, P. and Gmitro, M., Phys. Lett., **150B**, 50 (1985).
17. Gmitro, M. *et al.*, Nucl. Phys., **A453**, 685 (1986).
18. Heath, A.R. and Garvey, G.T., Phys. Rev., **C31**, 2190, (1985).
19. Huang, K. *et al.*, Phys. Rev. **108**, 1348 (1957).
20. Opat, G.I., Phys. Rev., **B428**, 134 (1964)
21. Hwang, W-Y.P. and Primakoff, H., Phys. Rev., **C18** 414 (1978).
22. Fearing, H.W., Phys. Rev., **C21**, 1951 (1980).
23. Beder, D.S. and Fearing, H.W., Phys. Rev. **D35**, 2130 (1987).
24. Blecher, M., *et al.*, *Measurement of the pseudoscalar coupling via radiative muon capture on hydrogen*, Proceedings of Panic '93 (INFN (1993)) pg. 171.